ISSN 0965-5441, Petroleum Chemistry, 2023, Vol. 63, No. 5, pp. 607–617. © The Author(s), 2023. This article is an open access publication.
ISSN 0965-5441, Petroleum Chemistry, 2023. © The Author(s), 2023. This article is an open access publication, corrected publication 2023.
Russian Text © The Author(s), 2023, published in Neftekhimiya, 2023, Vol. 63, No. 3, pp. 416–428.

Novel Samarium Cobaltate/Silicon Carbide Composite Catalyst for Dry Reforming of Methane into Synthesis Gas

A. S. Loktev[a,b,*], V. A. Arkhipova[a], M. A. Bykov[c], A. A. Sadovnikov[b], and A. G. Dedov[a,b]

[a] *Gubkin Russian State University of Oil and Gas (National Research University), Moscow, 119991 Russia*
[b] *Topchiev Institute of Petrochemical Synthesis, Russian Academy of Sciences, Moscow, 119991 Russia*
[c] *Faculty of Chemistry, Lomonosov Moscow State University, Moscow, 119991 Russia*
**e-mail: al57@rambler.ru; genchem@gubkin.ru*

Received October 31, 2022; revised February 7, 2023; accepted March 27, 2023

Abstract—The paper describes a specifically developed novel samarium cobaltate/silicon carbide composite that transforms into a high-performance carbon-resistant catalyst for dry reforming of methane into syngas (DRM). This 30%$SmCoO_3$/70%SiC composite without hydrogen prereduction was tested in DRM at atmospheric pressure and GHSV 15 L g^{-1} h^{-1} (of an equimolar CH_4–CO_2 mixture). During the test, the yields of hydrogen and carbon monoxide reached 92 and 91 mol %, respectively, at 900°C, and 20 and 28 mol % at 700°C. Using XRD, TGA, and SEM examination, zero carbonization of the catalyst surface was demonstrated. It was found that, in the course of DRM, the initial composite transformed into a material that contained silicon carbide, samarium silicate, and samarium oxide, as well as metallic cobalt nanoparticles (<20 nm).

Keywords: dry reforming of methane, synthesis gas, composite, samarium cobaltate, silicon carbide, carbon-resistant catalyst

DOI: 10.1134/S0965544123030052

Natural gas is extensively used as an easily transportable and environmentally friendly fuel. At the same time, its use in Russia as a raw material for the production of hydrogen and petrochemicals needs to be further promoted. This is in accordance with Priority 2 of the Strategy for Scientific and Technological Development of the Russian Federation; Priority 2 deals with, inter alia, improving the efficiency of deep processing of hydrocarbon raw materials and developing new energy sources and methods for transport and storage of energy.

In the production of hydrogen and petrochemicals from natural gas or from renewable sources such as biogas, the key process step is the production of synthesis gas (syngas, a CO–H_2 mixture). On an industrial scale, syngas and hydrogen are commonly produced by steam reforming of methane (SRM), an energy-consuming endothermic process that requires significant amounts of steam. Therefore, increasing attention has been paid to alternative syngas production approaches, specifically partial oxidation of methane (POM) [1–4] and dry reforming of methane (DRM) [1, 5–19].

POM has the advantages of exothermicity, high reaction rate, and a syngas composition (H_2 : CO = 2 : 1) suitable for further Fischer–Tropsch synthesis (FTS) of methanol and hydrocarbons without additional treatment. On the other hand, this process uses an explosive methane–oxygen mixture and requires costly facilities to be built for the production of pure oxygen.

Immense research has been devoted to DRM: over the period of 1990–2022, the number of publications on DRM exceeded one thousand, including 863 articles with more than six citations and 34 review articles [5]. In particular, recent reviews [5–19] offer an adequate presentation of the latest advances in the synthesis of high-performance carbon-resistant DRM catalysts, as well as an appropriate analysis of the current concepts regarding the thermodynamics, mechanisms, and kinetics of DRM reactions.

The tremendous interest in DRM is primarily motivated by its effective disposal of critical greenhouse gases, namely carbon dioxide and methane. Furthermore, an equimolar CO–H_2 mixture produced in this process is an advantageous intermediate for further production of hydrocarbons (by FTS) and a variety of oxygenates [1, 5–19]. The authors of [12] provide references to the potential uses of this gas mixture in various fuel components. Some reviews (e.g., [9]) consider syngas production by DRM a potential pathway to utilize solar or nuclear energy in chemical energy transmission systems. In addition, DRM catalysts allow syngas to be produced from biogas and other biomass and waste processing products [9, 12, 17, 18].

To date, DRM has mostly been implemented on a pilot scale in combination with SRM because adding CO_2 makes it possible to adjust the syngas composition and utilize the greenhouse gas [16, 18–20]. One example of steam-free DRM implementation is the CALCOR process [16, 18, 19, 21]. However, this process is aimed at preferential carbon monoxide synthesis (H_2 : CO = 0.42 : 1) and requires a large excess of CO_2.

The implementation of DRM itself has been constrained by a number of challenges, including high endothermicity (due to the stability of CO_2 and CH_4 molecules) and high propensity for coking and sintering of active catalytic sites (due to high process temperatures). Moreover, carrying out DRM at high pressures may also contribute to rapid carbonization; on the other hand, when syngas is produced at low pressures its subsequent processing generally requires a costly compression step to be installed [7, 9, 12, 16, 18, 22, 23].

Relevant thermodynamic calculations have determined optimal conditions for DRM (reaction 1): CO_2:CH_4=1:1, >850°C, and atmospheric pressure. These conditions ensure near-100% conversion of the reactants, H_2:CO=1:1, and mitigated carbonization (reaction 2) [11, 12, 14, 16, 19, 23]:

$$CH_4 + CO_2 \rightarrow 2CO + 2H_2;\ \Delta G^0_{298} \leq 0 \text{ at } T \geq 665°C, \quad (1)$$

$$CH_4 \leftrightarrow C + 2H_2;\ \Delta G^0_{298} \leq 0 \text{ at } T \geq 658°C. \quad (2)$$

Under these conditions, the reverse water–gas shift reaction (RWGSR, reaction 3), which affects both the product ratio and the CO_2 conversion, is thermodynamically allowed:

$$CO_2 + H_2 \leftrightarrow CO + H_2O;\ \Delta G^0_{298} \leq 0 \text{ at } T \geq 700°C. \quad (3)$$

At high temperatures, carbon may also form from the exothermic reactions of CO disproportionation and CO_2 hydrogenation [11].

Most publications on DRM discussed in [5–19] and other reviews have been focused specifically on the synthesis of stable and carbon-resistant DRM catalysts. The literature analysis presented in these reviews and, for example, in papers [24–33] suggests a number of major approaches to the synthesis of stable and carbon-resistant DRM catalysts:

1. Developing catalyst synthesis techniques that ensure the generation of nanosized metal active sites, including those with specific crystalline structures. This approach may involve a variety of solutions: loading of small amounts of metals on a support; preliminary synthesis and thermolysis of precursors based on perovskites, pyrochlores, spinels, hydrotalcites, etc.; addition of chelants; use of supports with well-developed surfaces; optimization of conditions for heat treatment and catalyst reduction; and other techniques;

2. Introducing alkaline promoters or using basic supports;

3. Generating oxygen vacancies on the support surface and using additives that supply active oxygen;

4. Using systems that provide strong metal–support interaction;

5. Using bimetallic systems that combine noble and non-noble metals (mostly nickel, cobalt, and platinum-group metals);

6. Synthesizing core–shell catalysts by encapsulating active metal sites in a gas-permeable oxide shell; and

7. Partial poisoning of the active catalytic sites.

In most cases, known DRM catalysts with both good stability and high productivity were manufactured by a combination of the approaches listed above. Given that dissociative adsorption of methane is commonly held to be the rate-limiting step in DRM, these approaches are intended both to avoid the sintering of active sites and to preclude the generation of stable surface carbon forms such as graphite, carbon fibers, or nanotubes (because their generation deactivates the active sites, destroys the catalyst, and blocks the passage of gases through the reactor). On the other hand, a positive effect of surface carbon on DRM performance has also been reported [32].

In previous studies, we prepared a perovskite-structured samarium cobaltate by thermal decomposition of a specifically synthesized heterometallic cobalt–samarium

complex $(Co(phen)_3][Sm(NO_3)_5(H_2O)]\cdot 2MeCN$ (where phen is *o*-phenanthroline, and MeCN is methyl acetate). This samarium cobaltate effectively catalyzed both POM and DRM as it transformed in situ into a composite that contained metallic cobalt dispersed in a Sm_2O_3 matrix [34, 35]. However, during the DRM, a significant amount of carbon was formed on the surface of this composite, thus even blocking the gas flow in the reactor, despite the thermodynamically favorable DRM conditions. The carbonization of this catalyst was finally mitigated by using a sophisticated procedure for supercritical antisolvent precipitation (SAS) of the perovskite precursor complex, and this diminished the particles of the target $SmCoO_3$ catalyst for DRM and POM.

Deposition of perovskite precursors on various supports is known to facilitate the preparation of more stable DRM catalysts [6, 9, 13, 19].

Grinding a mesoporous SBA-15 material with nickel nitrate proved to be a simple and effective method for the synthesis of a carbon-resistant Ni-SBA-15 catalyst for DRM [29].

The preparation of high-performance DRM catalysts using silicon carbide was described in [26, 37]. The authors of [26] used β-SiC coated with $CeZrO_2$ as a support for Ni–Co active sites. A similar approach was followed in [37] for the synthesis of a Ni/CeO_2–CDC–SiC catalyst for DRM (where CDC is carbide-derived carbon, i.e., surface carbon formed from silicon carbide).

Silicon carbide, a chemically stable and highly heat-conductive material, has been extensively used as an inert support for heterogeneous catalysts [36]. The high thermal conductivity of silicon carbide provides a uniform temperature profile across the catalyst bed, thus preventing hot spots and, hence, protecting the catalyst from carbonization and active-site sintering [26, 37]. However, to the best of our knowledge, there are no available references on the synthesis of DRM and POM catalysts by dispersing perovskites in a silicon carbide matrix.

The purpose of the present study was to develop and test, both in DRM and POM, a simpler novel approach to mitigating the carbonization of a $SmCoO_3$-derived catalyst synthesized by thermolysis of a metal complex precursor. This catalyst synthesis approach involves an uncomplicated procedure for mechanical dispersion of $SmCoO_3$ with excess silicon carbide.

EXPERIMENTAL

Samarium cobaltate was synthesized by thermal decomposition, at 800°C, of a heterometallic cobalt–samarium complex similar to that used in [34, 35]. The synthesis technique and properties of the parent complex are described in [38].[1] The procedures for thermal decomposition of the complex to produce samarium cobaltate ($SmCoO_3$) and for characterization of $SmCoO_3$ are similar to those described in [34, 35]. The XRD showed that the synthesized $SmCoO_3$ was a single-phase perovskite material with a specific surface area (S_{BET}) of 5 m^2/g.

A mixture of samarium cobaltate and silicon carbide was dispersed in a SPEX 800 Mixer/Mill ball mill (SPEX SamplePrep, USA) over a period of 1 h, using a container and balls made of tungsten carbide. The container was loaded with silicon carbide (SiC 1-S2/3-M β-SiC 2–3 mm spherical, SICAT, Germany, S_{BET} = 29.4 m^2/g) and a samarium cobaltate powder (30% by weight of the resultant composite).

The prepared dispersed powder (S_{BET} = 33.6 m^2/g) was pressed into pellets, which were then crushed to 0.5–1 mm grain size. This catalyst is hereinafter designated as $30\%SmCoO_3/SiC$.

The phase compositions both of the fresh and spent catalysts were identified by X-ray diffraction (XRD) on a Rigaku MiniFlex 600 diffractometer (CuK_α radiation, λ = 1.54187 Å) using database of the International Center for Diffraction Data (ICDD).

The specific surface areas (S_{BET}) were measured by low-temperature nitrogen adsorption using the Brunauer–Emmett–Teller (BET) five-point method at relative partial pressures (P/P_0) of 0.05–0.25 using an *ATKh-06* sorption analyzer (Katakon, Russia).

Thermogravimetric analysis (TGA) of the spent catalyst was performed in an air flow under heating from 35 to 900°C at a rate of 10°C/min. The TGA data were processed using the NETZSCH Proteus Thermal Analysis software package.

The spent catalyst was examined by scanning electron microscopy (SEM) on a Carl Zeiss NVision 40 microscope at magnification up to ×200 000 using SE or

[1] The authors thank A.V. Gavrikov, PhD (Chem.), Senior Researcher at Kurnakov Institute of General and Inorganic Chemistry of the Russian Academy of Sciences, who synthesized and provided the parent complex.

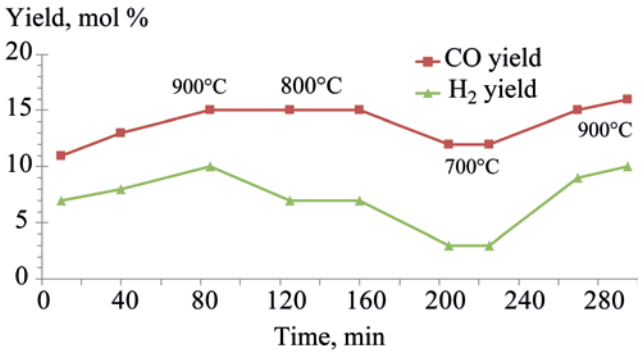

Fig. 1. Yields from POM for 30%$SmCoO_3$/SiC catalyst.

InLens secondary electron detectors (accelerating voltage 7 kV) and ESB backscattered detectors (accelerating voltage 1 kV). The microscope was equipped with an Oxford Instruments X-MAX 80 mm detector with an accelerating voltage of 1–20 kV to measure the elemental composition of samples by X-ray microanalysis.

The spent catalyst was further examined by transmission electron microscopy (TEM) on a JEOL JEM-2100 microscope (accelerating voltage 200 kV, cell resolution 0.19 nm). The microscope was equipped with an Olympus Quemesa 11 camera and an EX-24065JGT energy dispersive analyzer. The samples were treated with ethanol and deposited on a copper grid (Ted Pella, Inc.)[2].

Both the fresh and spent catalysts were subjected to temperature-programmed reduction in hydrogen (H_2-TPR) in a flow-type quartz reactor (inner diameter 2 mm) under heating at a rate of 7.5°C/min in a 5%H_2/Ar flow (50 mL/min). The samples weighed 50 mg. The hydrogen content was identified using a *Crystal Lux 4000M* chromatograph equipped with a thermal conductivity detector.[3]

The POM and DRM reactions were carried out in a vertical heated flow-type quartz reactor (inner diameter 18 mm) with an axial thermocouple pocket (outer diameter 8 mm). The tip of the chromel–alumel K-type thermocouple was located in the middle of the catalyst bed. The catalyst (0.2 g, 0.5–1 mm grain, 1 mm bed) was placed on a quartz fiber support. For POM, the free reactor volume was filled with quartz chips. The catalyst was heated to 900°C in a flow of CH_4–CO_2 or CH_4–O_2 mixtures undiluted with an inert gas (CP grade, 99.9%; the Moscow Gas Processing Plant, Russia; $CH_4/CO_2 = 1$; $CH_4/O_2 = 2$), the mixtures being injected to the reactor top. The gas mixture flow rate was 12 liters per gram catalyst per hour (L g^{-1} h^{-1}) for POM and 15 L g^{-1} h^{-1} for DRM. At a set temperature point, the gas flow rates to and from the reactor were measured, and both the initial mixtures and products were analyzed, after which the temperature was adjusted to other setpoints without stopping the gas injection.

The reaction products were analyzed by a GC method similar to that described in [34, 35]. The conversion of methane, oxygen, and carbon dioxide, as well as the hydrogen and CO yields (in mol %), were derived from the equations described in [34, 35, 39] based on the GC data for the initial mixtures and reaction products. The calculations took into account the moles of hydrogen and carbon atoms in the gas feed and in the products.

RESULTS AND DISCUSSION

The choice of POM and DRM test conditions was primarily motivated by the need to correctly compare the performance exhibited by the novel catalyst with the test data on POM [34] and DRM [35] over SiC-free samarium cobaltate. These conditions were basically similar to those reported in many other publications on POM and DRM, including the reactions carried out in the presence of rare-earth (REE) nickelates and cobaltates. A literature review on the application of perovskite-based and other catalysts in POM and DRM reveals that the gas hourly space velocities (GHSV) of reactants vary over a wide range of 1 to 1000 L g^{-1} h^{-1}. The reactants are often diluted with an inert gas. The GHSV of the undiluted reactants used in our study eliminated any diffusion limitations and caused no pressure drop across the reactor; moreover, these velocities enabled us to estimate the catalyst performance under significant feed rates. Detailed investigation of the effects of the space velocity and ratio of reactants on the POM and DRM performance fell beyond the scope of this work and probably needs further research.

Figure 1 illustrates the test data for 30%$SmCoO_3$/SiC in POM at 700–900°C. It clearly indicates that the yields of CO and H_2 amounted to 11–16 and 3–10 mol %, respectively, with CH_4 conversion of 31–34% and near-quantitative oxygen conversion.

[2] The authors thank K.A. Cherednichenko, PhD (Chem.), Senior Researcher at Gubkin University, for help with the TEM examination.

[3] The authors thank A.E. Sotnikova, Junior Researcher at TIPS RAS, for help with the temperature-programmed reduction of the samples.

It is known, however, that in POM over SiC-free $SmCoO_3$, near-100% conversion of CH_4 and O_2 and near-100% yields of CO and H_2 can be achieved already after initial heating to 900°C [34]. Even at 750°C, the yields of CO and H_2 remained high (65 mol %). Therefore, 30%$SmCoO_3$/SiC, the catalyst in which silicon carbide accounted for 70%, exhibited a markedly lower performance in POM than the 100% samarium cobaltate catalyst studied in [34]. This may be associated not only with the lower amount of perovskite in the precursor but also with potential oxidation of silicon carbide by the oxygen contained in the methane–oxygen mixture injected to the reactor. The subsequent interaction between the newly-formed silicon oxide and samarium cobaltate could form cobalt silicate, a compound resistant to reduction and catalytically inefficient. The XRD pattern of the spent catalyst after POM completely lacked peaks intense enough to be identified, thus indicating the formation of an amorphous material inefficient in POM.

In the DRM tests, where the feed consisted of a CH_4–CO_2 mixture (i.e., oxygen-free, unlike the POM feed), the 30%$SmCoO_3$/SiC catalyst exhibited high performance in syngas production (Fig. 2). After the catalyst was heated to 900°C, the CH_4 and CO_2 conversion reached 84 and 91%, respectively, and the yields of CO and H_2 amounted to 81 and 80 mol %, respectively.

Subsequent cooling to 800°C led to a decrease in the CO and H_2 yields to 63–66 and 52–56 mol %, respectively. At 700°C the CO and H_2 yields dropped to 28 and 20 mol %, respectively. The significant amount of water formed during the cooling and the excess of CO yields over hydrogen yields can likely be explained by an increased contribution of RWGSR (3) to the formation of the target products.

Although at 600°C only trace amounts of syngas were formed, subsequent reheating of the catalyst to 900°C saw its syngas production performance recover. The CO and H_2 yields (91 and 92 mol %, respectively) exceeded the values observed during the initial heating to 900°C, indicating an increased performance of the catalyst in DRM after the reheating to 900°C.

It should be noted that, under similar DRM conditions, the SiC-free samarium cobaltate catalyst exhibited CH_4 conversion of 97–99%, CO_2 conversion of 95–96%, a CO yield of 90–93 mol %, and a H_2 yield of 91–95 mol % as soon as the catalyst was heated to 800°C in the CH_4–CO_2 mixture [35]. At 900°C the product yields reached 98–100 mol %, after which the reactor was

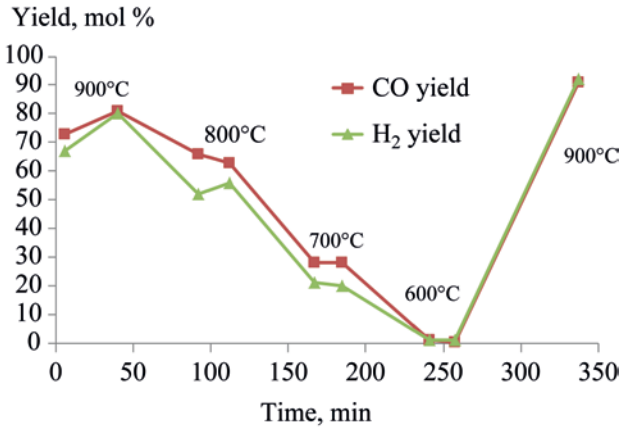

Fig. 2. Yields from DRM for 30%$SmCoO_3$/SiC catalyst.

blocked by carbon deposits. The TGA examination of the spent catalyst showed a 49% weight loss attributable to the combustion of carbon deposits [ibid].

A comparison of the DRM data reported in [35] with the results of the present study shows that, at 900°C and GHSV 15 L g^{-1} h^{-1} (of the equimolar CH_4–CO_2 feed mixture), the 30%$SmCoO_3$/SiC catalyst was only slightly inferior to the 100%$SmCoO_3$ catalyst in terms of product yields, despite the substantially lower $SmCoO_3$ content in the 30%$SmCoO_3$/SiC.

The findings reported in [35] as well as in some other works demonstrate that, in DRM, $SmCoO_3$-based catalysts transform into composites that contain metallic cobalt particles dispersed in a samarium oxide matrix. The metallic cobalt particles are the key component that catalyzes DRM. In this context, it is important that the novel 30%$SmCoO_3$/SiC catalyst exhibited CO and H_2 productivity of 512 moles per gram-atom of Co per hour (mol g-at^{-1} h^{-1}), compared to 160 mol g-at^{-1} h^{-1} or lower as reported for the 100%$SmCoO_3$ catalyst [35]. Therefore, the dispersion of samarium cobaltate in silicon carbide led to a threefold increase in the performance of the cobalt active sites generated during DRM in terms of syngas productivity. Moreover, during the reactions over the novel 30%$SmCoO_3$/SiC catalyst, the reactor was not blocked by carbon.

The XRD powder pattern of the post-DRM 30%$SmCoO_3$/SiC catalyst (Fig. 3) displays a composite that consists (as evaluated by the Rietveld method) of 32 mol % $Sm_5Si_3O_{13}$ (samarium silicate), 63 mol % SiC (silicon carbide), 4 mol % metallic cobalt, and only

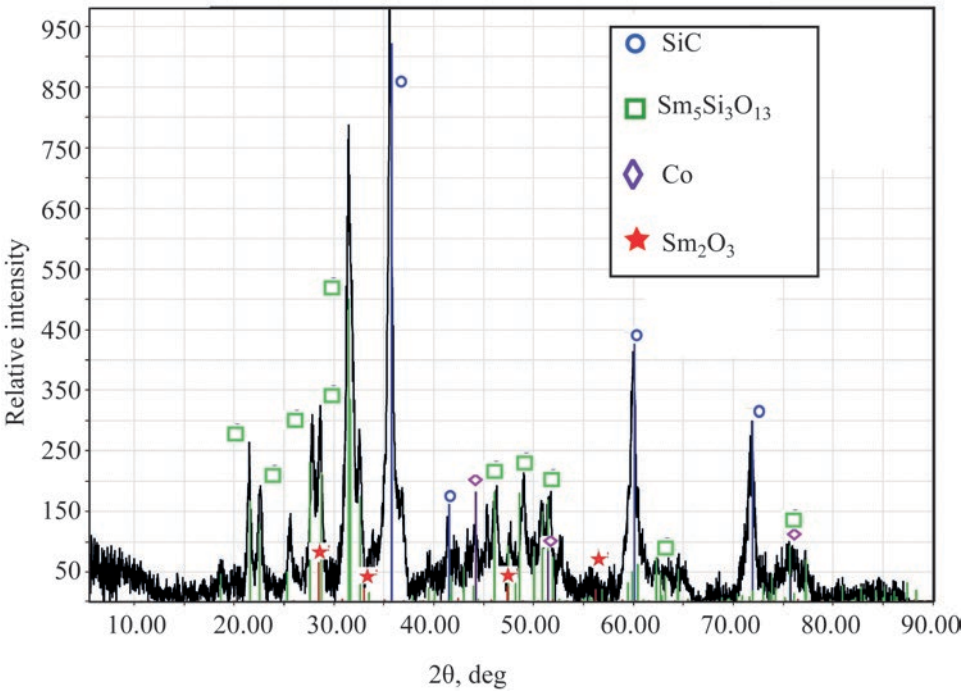

Fig. 3. XRD powder pattern of spent 30%$SmCoO_3$/SiC catalyst after DRM.

1 mol % Sm_2O_3—the true DRM catalyst generated in the reactor. The catalyst discharged from the reactor had pronounced ferromagnetic properties, probably due to the significant presence of metallic cobalt. No other ferromagnetic components were detected by XRD. The broad low-intensity peak of metallic cobalt in the XRD pattern points to the small size of its particles, thus limiting the application of the Scherrer equation.

The TGA data for the spent 30%$SmCoO_3$/SiC catalyst after DRM are illustrated in Fig. 4. The spent catalyst exhibited a slight weight loss under heating in air from 100 to 350°C due to water desorption, and a minor weight increase between 350 and 520°C resulting from the oxidation of metallic cobalt. The 3% weight loss between 540 and 750°C was attributable both to the combustion of a small amount of carbonaceous deposits and the decomposition of $Sm_2(CO_3)_3$ (samarium carbonate) and $(SmO)_2CO_3$ (samarium oxycarbonate).

The potential minor surface carbonization may, to an extent, have been caused not only by the transformations of the CH_4–CO_2 mixture components but also by the partial conversion of silicon carbide to samarium silicate (as actually detected).

The weight increase of the spent catalyst sample above 740°C (see Fig. 4) may be attributable both to the oxidation of silicon carbide into silicon oxide and to the interaction of cobalt oxide and samarium oxide with atmospheric oxygen to form samarium cobaltate:

$$4Co_3O_4 + O_2 + 6Sm_2O_3 \rightarrow 12SmCoO_3. \quad (4)$$

Figure 5 presents the SEM and TEM images of the spent DRM catalyst recorded in secondary electrons (Fig. 5a) and backscattered electrons (Fig. 5b). Figure 5a shows aggregates of uniformly distributed 50–100 nm particles. The backscattered electron micrograph (Fig. 5b) indicates uniformly distributed light particles, apparently samarium compounds. At the same time, the catalyst surface micrographs lack any evidence of surface carbonization.

The distribution of chemical elements on the catalyst surface (Figs. 5c, 5d) demonstrates the location of significant amounts of samarium and cobalt on the surface of silicon carbide, as well as a noticeable coincidence of the location regions of cobalt, samarium, and silicon atoms. The high-resolution micrograph (Fig. 5e) indicates the presence of cobalt nanoparticles (<20 nm) in the spent catalyst.

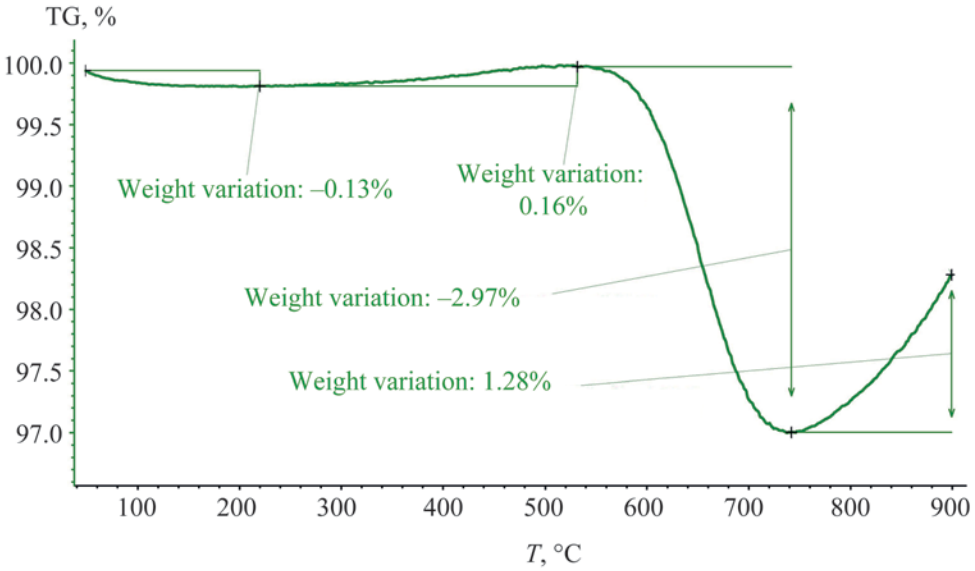

Fig. 4. TGA data for spent 30%$SmCoO_3$/SiC catalyst after DRM.

Both the fresh and spent DRM catalysts were further examined by H_2-TPR (Fig. 6). The hydrogen absorption regions of these catalysts correspond to the following reactions, typical of the reduction of $SmCoO_3$ [40] and other similar perovskites [6]:

$$2SmCoO_3 + H_2 \rightarrow 2SmCoO_{2.5} + H_2O \quad (5)$$

280–480°C,

$$2SmCoO_{2.5} + 2H_2 \rightarrow Sm_2O_3 + 2Co + 2H_2O \quad (6)$$

480–580°C.

Although similar hydrogen absorption ranges were previously observed in H_2-TPR of samarium cobaltate synthesized by the citrate method [41], the second peak had a shoulder. This led the researchers to suggest the formation of an equimolar Sm_2CoO_4/CoO mixture (corresponding to the composition of $SmCoO_{2.5}$) and the further reduction of these products within close temperature ranges.

A comparison of Figs. 6a and 6b shows that the spent catalyst may also contain samarium cobaltate, while the more intense peak (Fig. 6b) is ascribed to the product of $SmCoO_3$ reduction by reaction (5). The lack of $SmCoO_3$ reflections in the XRD pattern of the spent catalyst (see Fig. 3) can be explained by the overly small amount of $SmCoO_3$ or the overly small size of its particles.

Thus, within the scope of this study, the 30% samarium cobaltate synthesized by thermolysis of the unconventional precursor—specifically, the heterometallic complex $[Co(phen)_3][Sm(NO_3)_5(H_2O)]\cdot 2MeCN$ (with *o*-phenanthroline as a ligand)—was dispersed in a silicon carbide matrix. This technique enabled us to prepare a material that transformed, under DRM process conditions, into a carbon-resistant catalyst that achieved a high syngas yield (above 90%). Although the previously investigated materials, namely the SiC-free samarium cobaltate synthesized by a similar manner [35] and the samarium cobaltate prepared by the citrate method [41], also exhibited high yields of syngas, they were prone to carbonization due to their substantially larger content of perovskite. In the DRM test, the novel 30%$SmCoO_3$/SiC catalyst exhibited CO and H_2 productivity of 512 mol g-at^{-1} h^{-1}, i.e. the values significantly exceeding the productivity of identical components reported for the 100%$SmCoO_3$ catalyst.

The DRM catalyst generated from the composite prepared in this study consisted of small (<20 nm) cobalt particles that provided higher syngas productivity. Apparently, the smaller size of these particles prevented them from being involved in carbonization in the form of fibers, nanotubes, and other carbon deposits. The presence of silicon carbide provides a uniform temperature profile across the catalyst bed, thus improving the carbon resistance of the catalyst and the sintering resistance of

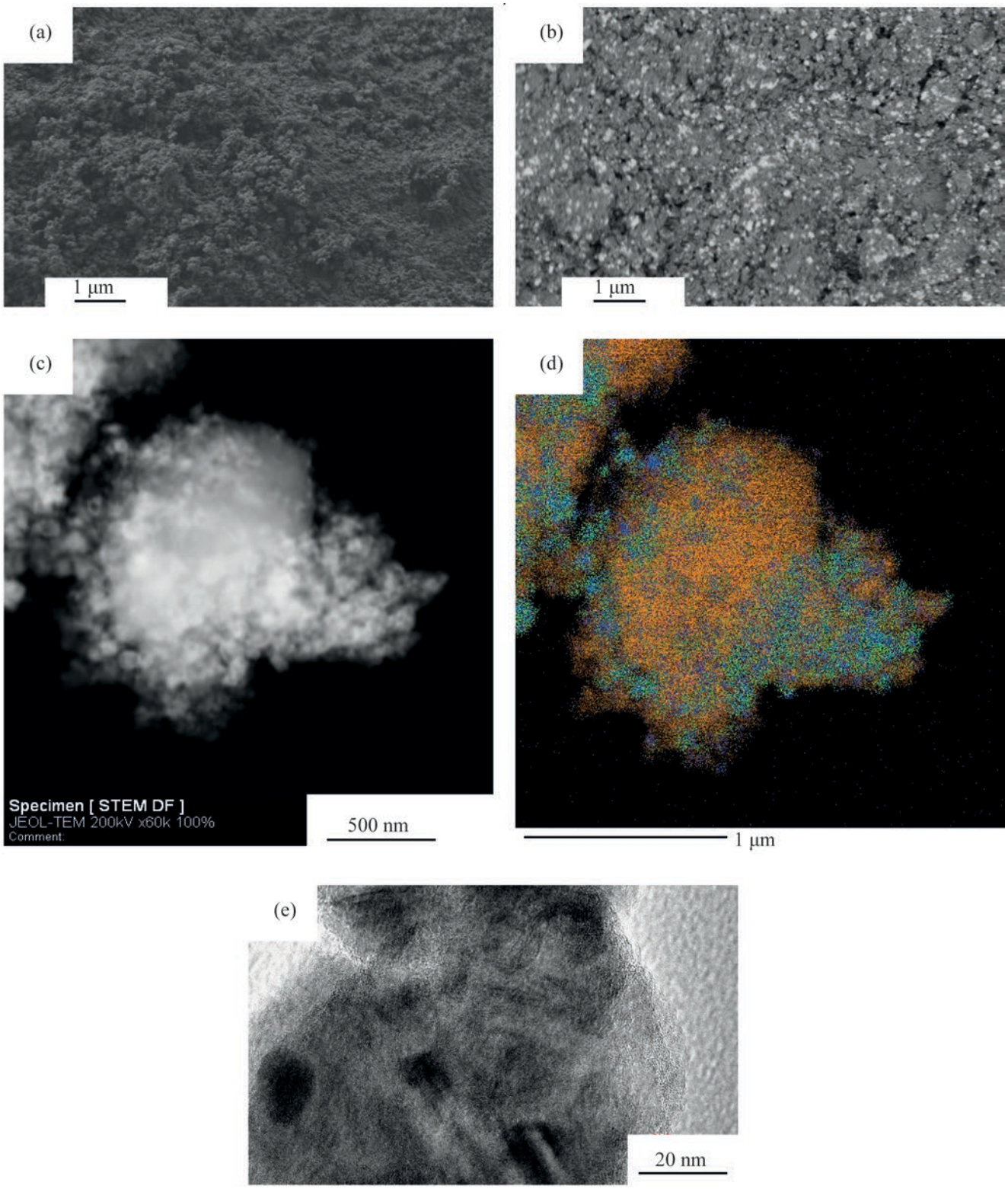

Fig. 5. Micrographs and element distribution in 30%$SmCoO_3$/SiC catalyst after DRM: (a) secondary electron SEM micrograph; (b) backscattered electron SEM micrograph; (c) TEM micrograph of catalyst particle; (d) the same TEM micrograph with color indication of element distribution: orange for Si, blue for Co, and green for Sm; (e) high-precision TEM micrograph.

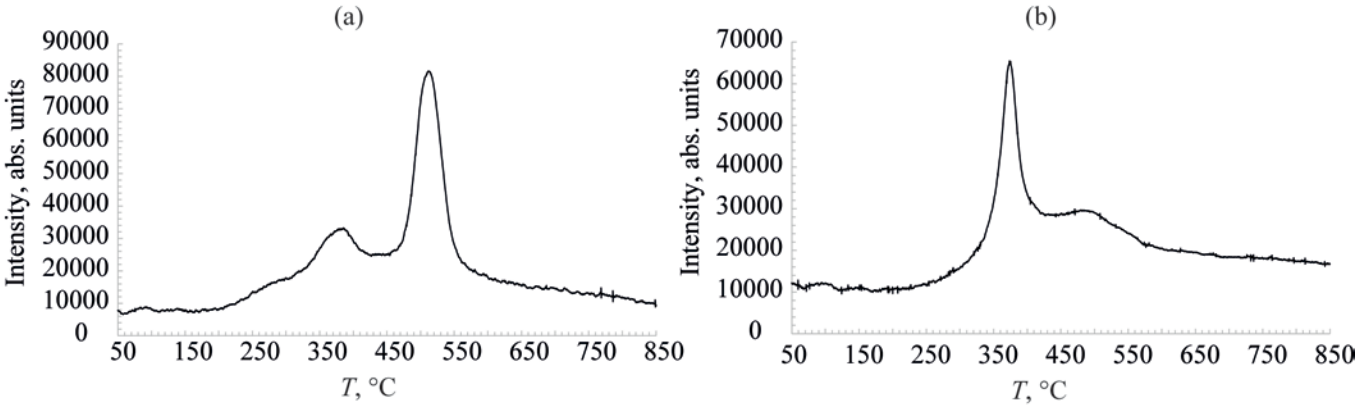

Fig. 6. H_2-TPR data for 30%$SmCoO_3$/SiC catalyst: (a) fresh; (b) spent after DRM.

the cobalt particles. Moreover, it is reasonable to assume that the detected formation of the samarium silicate phase also contributed to the catalyst's better resistance to carbonization and sintering, probably due to the strong metal–support interaction. This contribution is consistent with the substantial coincidence of the cobalt, samarium, and silicon location regions. However, this assumption needs further research. Importantly, unlike many known carbon-resistant DRM catalysts, the novel catalyst was free of strongly basic components and suppliers of active oxygen, and was not marked by a developed specific surface.

In general, the proposed approach might also prove effective for enhancing the carbon resistance of various REE–Co(Ni)O_3 perovskites in DRM.

CONCLUSIONS

The paper describes a novel approach to synthesizing a high-performance carbon-resistant catalyst for dry reforming of methane into syngas. According to this approach, a perovskite material, namely samarium cobaltate, synthesized by thermolysis of specifically synthesized heterometallic complex $[Co(phen)_3][Sm(NO_3)_5(H_2O)]\cdot 2MeCN$ (with *o*-phenanthroline as a ligand), is mechanically dispersed with silicon carbide. The resultant 30%$SmCoO_3$/70%SiC composite, without prior hydrogen reduction, was tested in DRM at atmospheric pressure and GHSV 15 L g^{-1} h^{-1} (the feed consisted of an equimolar CH_4–CO_2 mixture). During the test, the yields of hydrogen and carbon monoxide reached 92 and 91 mol %, respectively, at 900°C, and 20 and 28 mol % at 700°C. These values are comparable to the yields reported for a 100% samarium cobaltate and other high-performance DRM catalysts. Using XRD, TGA, and SEM examination, zero carbonization of the catalyst surface was demonstrated. It was found that, in the course of DRM, the initial composite transformed into a material that contained silicon carbide, samarium silicate, and samarium oxide, as well as metallic cobalt nanoparticles (<20 nm). The significant content of silicon carbide in the catalyst makes it possible to reduce the catalyst cost and maintain a uniform temperature profile across the catalyst bed in future larger-scale testing. The comparatively high syngas yields and carbon resistance can be explained by the small size of cobalt particles and by the generation of a samarium silicate phase that stabilizes cobalt active sites. Provided that the larger-scale test of the novel catalyst proves successful, this catalyst can be recommended for practical implementation in DRM.

AUTHOR INFORMATION

A.S. Loktev, ORCID: https://orcid.org/0000-0002-5841-8085

V.A. Arkhipova, ORCID: https://orcid.org/0000-0002-2751-4840

M.A. Bykov, ORCID: https://orcid.org/0000-0002-5000-9199

A.A. Sadovnikov, ORCID: https://orcid.org/0000-0002-3574-0039

A.G. Dedov, ORCID: https://orcid.org/0000-0001-8086-2345

ACKNOWLEDGMENTS

This work was performed using equipment of the Shared Research Center "Analytical center of deep oil processing and petrochemistry" of TIPS RAS. The authors thank the Joint Research Center for Physical Methods of Research at Kurnakov Institute of General and Inorganic Chemistry of the Russian Academy of Sciences (JRC PMR IGIC RAS) for their cooperation in the investigation of catalyst properties.

FUNDING

The study described here was performed with financial support from the Russian Science Foundation (Grant no. 20–13–00138: catalyst synthesis) and within the State Program of TIPS RAS (catalytic test and catalyst characterization).

CONFLICT OF INTEREST

A.G. Dedov, a co-author, is an editorial board member at the Neftekhimiya (Petroleum Chemistry) Journal. The other co-authors declare no conflict of interest requiring disclosure in this article.

REFERENCES

1. Holmen, A., *Catal. Today*, 2009, vol. 142, pp. 2–8. https://doi.org/10.1016/j.cattod.2009.01.004
2. Dedov, A.G., *Her. Russ. Acad. Sci*., 2016, vol. 86, no. 3, pp. 234–241. https://doi.org/10.1134/S1019331616030023
3. Elbadawi, A.H., Ge, L., Li, Z., Liu, S., Wang, S., and Zhu, Z., *Catal. Rev*., 2021, vol. 63, pp. 1–67. https://doi.org/10.1080/01614940.2020.1743420
4. Moiseev, I.I., Loktev, A.S., Shlyakhtin, O.A., Mazo, G.N., and Dedov, A.G., *Petrol. Chem.*, 2019, vol. 59, pp. S1–S20. https://doi.org/10.1134/S0965544119130115
5. Alhassan, M., Jalil, A.A., Nabgan, W., Hamid, M.Y.S., Bahari, M.B., and Ikram, M., *Fuel*, 2022, vol. 328, p. 125240. https://doi.org/10.1016/j.fuel.2022.125240
6. Bhattar, S., Abedin, Md.A., Kanitkar, S., and Spivey, J.J., *Catal. Today*, 2021, vol. 365, pp. 2–23. https://doi.org/10.1016/j.cattod.2020.10.041
7. Jang, W.-J., Shim, J.-O., Kim, H.-M., Yoo, S.-Y., and Roh, H.-S., *Catal. Today*, 2019, vol. 324, pp. 15–26. https://doi.org/10.1016/j.cattod.2018.07.032
8. Zhang, G., Liu, J., Xu, Y., and Sun, Y., *Int. J. Hydrogen Energy*, 2018, vol. 43, no. 32, pp. 15030–15054. https://doi.org/10.1016/j.ijhydene.2018.06.091
9. Usman, M., Wan Daud, W.M.A., and Abbas, H.F., *Ren. Sustain. Energy Rev.*, 2015, vol. 45, pp. 710–744. https://doi.org/10.1016/j.rser.2015.02.026
10. Makaryan, I.A., Sedov, I.V., Nikitin, A.V., and Arutyunov, V.S., *Nauch. Zh. Ross. Gaz. O–va*, 2020, no. 1 (24), pp. 50–68.
11. Teh, L.P., Setiabudi, H.D., Timmiati, S.N., Aziz, M.A.A., Annuar, N.H.R., and Ruslan, N.N., *Chem. Eng. Sci*., 2021, vol. 242. I. 116606. https://doi.org/10.1016/j.ces.2021.116606
12. Yentekakis, I.V., Panagiotopoulou, P., and Artemakis G., *Appl. Catal. B: Environ*., 2021, vol. 296. I. 120210. https://doi.org/10.1016/j.apcatb.2021.120210
13. Wang, C., Wang, Y., Chen, M., Liang, D., Yang, Z., Cheng, W., Tang, Z., Wang, J., and Zhang, H., *Int. J. Hydrogen Energy*, 2021, vol. 46, no. 7, pp. 5852–5874. https://doi.org/10.1016/j.ijhydene.2020.10.240
14. Yusuf, M., Farooqi, A.S., Keong, L.K., Hellgardt, K., and Abdullah, B., *Chem. Eng. Sci*., 2021, vol. 229, p. 116072. https://doi.org/10.1016/j.ces.2020.116072
15. Guharoy, U., Reina, T.R., Liu, J., Sun, Q., Gu, S., and Cai, Q., *J. CO_2 Util*., 2021, vol. 53, p. 101728. https://doi.org/10.1016/j.jcou.2021.101728
16. Baharudin, L., Rahmat, N., Othman, N.H., Shah, N., and Syed-Hassan, S.S.A., *J. CO_2 Util*., 2022, vol. 61, p. 102050. https://doi.org/10.1016/j.jcou.2022.102050
17. Gao, Y., Jiang, J., Meng, Y., Yan, F., and Aihemaiti, A., *Energy Convers. Managem*., 2018, vol. 171, pp. 133–155. https://doi.org/10.1016/j.enconman.2018.05.083
18. le Saché, E. and Reina, T.R., *Progr. Energy Combust. Sci*., 2022, vol. 89, p. 100970. https://doi.org/10.1016/j.pecs.2021.100970

19. Hambali, H.U., Jalil, A.A., Abdulrasheed, A.A., Siang, T.J., Gambo, Y., and Umar, A.A., *Int. J. Hydrogen Energy*, 2022, vol. 47, no. 72, pp. 30759–30787. https://doi.org/10.1016/j.ijhydene.2021.12.214
20. Mortensen, P.M. and Dybkjær, I., *Appl. Catal. A: General*, 2015, vol. 495, pp. 141–151. https://doi.org/10.1016/j.apcata.2015.02.022
21. Teuner, S.C., Neumann, P., and Linde, F.V., *Erdol Erdgas Kohle*, 2001, vol. 117, no. 12, pp. 580–582.
22. Schulz, L.A., Kahle, L.C.S., Delgado, K.H., Schunk, S.A., Jentys, A., Deutschmann, O., and Lercher, J.A., *Appl. Catal. A: General*, 2015, vol. 504, pp. 599–607. https://doi.org/10.1016/j.apcata.2015.03.002
23. Jang, W.-J., Jeong, D.-W., Shim, J.-O., Kim, H.-M., Roh, H.-S., Son, I.H., and Lee, S.J., *Appl. Energy*, 2016, vol. 173, pp. 80–91. https://doi.org/10.1016/j.apenergy.2016.04.006
24. Horiuchi, T., Sakuma, K., Fukui, T., Kubo, Y., Osaki, T., and Mori, T., *Appl. Catal. A: General*, 1996, vol. 144, nos. 1–2, pp. 111–120. https://doi.org/10.1016/0926-860X(96)00100-7
25. Gould, T.D., Izar, A., Weimer, A.W., Falconer, J.L., and Medlin, J.W., *ACS Catal*., 2014, vol. 4, pp. 2714–2717. https://doi.org/10.1021/cs500809w
26. Aw, M.S., Zorko, M., Djinović, P., and Pintar, A., *Appl. Catal. B: Environ*., 2015, vol. 164, pp. 100–112. https://doi.org/10.1016/j.apcatb.2014.09.012
27. Wang, Y.-H., Liu, H.-M., and Xu, B.-Q., *J. Mol. Catal. A: Chem*., 2009, vol. 299, pp. 44–52. https://doi.org/10.1016/j.molcata.2008.09.025
28. Wang, F., Han, B., Zhang, L., Xu, L., Yu, H., and Shi, W., *Appl. Catal. B: Environ*., 2018, vol. 235, pp. 26–35. https://doi.org/10.1016/j.apcatb.2018.04.069
29. Zhang, Q., Zhang, T., Shi, Y., Zhao, B., Wang, M., Liu, Q., Wang, J., Long, K., Duan, Y., and Ning, P., *J. CO_2 Util*., 2017, vol. 17, pp. 10–19. https://doi.org/10.1016/j.jcou.2016.11.002
30. Chong, C.C., Bukhari, S.N., Cheng, Y.W., Setiabudi, H.D., Jalil, A.A., and Phalakornkule, C., *Appl. Catal. A: General*, 2019, vol. 584. I. 117174. https://doi.org/10.1016/j.apcata.2019.117174
31. Han, K., Yu, W., Xu, L., Deng, Z., Yu, H., and Wang, F., *Fuel*, 2021, vol. 291. I. 120182. https://doi.org/10.1016/j.fuel.2021.120182
32. Wang, D., Littlewood, P., Marks, T.J., Stair, P.C., and Weitz, E., *ACS Catal*., 2022, vol. 12, no. 14, pp. 8352–8362
33. Schrenk, F., Lindenthal, L., Drexler, H., Urban, G., Rameshan, R., Summerer, H., Berger, T., Ruh, T., Opitz, A.K., and Rameshan, C., *Appl. Catal. B: Environ*., 2022, vol. 318, p. 121886. https://doi.org/10.1016/j.apcatb.2022.121886
34. Gavrikov, A.V., Loktev, A.S., Ilyukhin, A.B., Mukhin, I.E., Bykov, M.A., Vorobei, A.M., Parenago, O.O., Cherednichenko, K.A., Sadovnikov, A.A., and Dedov, A.G., *Int. J. Hydrogen Energy*, 2023, vol. 48, no. 8, pp. 2998–3012. https://doi.org/10.1016/j.ijhydene.2022.10.068
35. Gavrikov, A.V., Loktev, A.S., Ilyukhin, A.B., Mukhin, I.E., Bykov, M.A., Maslakov, K.I., Vorobei, A.M., Parenago, O.O., Sadovnikov, A.A., and Dedov, A.G., *Dalton Transact*., 2022, vol. 51, pp. 18446–18461. https://doi.org/10.1039/D2DT03026H
36. Westphalen, G., Baldanza, M.A.S., de Almeida,, A.J., Salim, V.M.M., da Silva, M.A.P., and da Silva, V.T., *Catal. Lett*., 2022, vol. 152. P., 2056–2066.
37. Guo, Y., Zou, J., Shi, X., Rukundo, P., and Wang, Z.-J., *ACS Sustain. Chem. Eng*., 2017, vol. 5, pp. 2330–2338. https://doi.org/10.1021/acssuschemeng.6b02661
38. Gavrikov, A.V., Ilyukhin, A.B., Belova, E.V., Yapryntsev, A.D., Dobrokhotova, Z.V., Khrushcheva, A.V., and Efimov, N.N., *Ceram. Int*., 2020, vol. 46, pp. 13014–13024. https://doi.org/10.1016/j.ceramint.2020.02.071
39. Loktev, A.S., Arkhipova, V.A., Bykov, M.A., Sadovnikov, A.A., and Dedov, A.G., *Petrol. Chem.*, 2023. https://doi.org/10.1134/S0965544123010048
40. Ma, F., Chen, Y., and Lou, H., *React. Kinet. Catal. Lett*., 1986, vol. 31, no. 1, pp. 47–53.
41. Osazuwa, O.U. and Cheng, C.K., *J. Clean Prod*., 2017, vol. 148, pp. 202–211. https://doi.org/10.1016/j.jclepro.2017.01.177